Analysis of the Defect-Irrelevant behavior of a No-Insulation HTS pancake coil including multiple superconductive joints

A. Musso[1], J. Bang[2], U. Bong[2], M. Breschi[1], C. Im[2], G. Kim[2], J. Kim[2], J. Park[2] and S. Hahn[2]

[1]University of Bologna, Italy
[2]Seoul National University, Republic of Korea

서울대학교
SEOUL NATIONAL UNIVERSITY

MT27
27th International Conference on Magnet Technology (MT27)
Fukuoka, Japan / 2021

Outline

- Introduction
- Experimental set-up
  - Superconducting joints
  - Winding and instrumentation phases
- Coil tests
  - Charge-discharge cycles
  - Rapid discharge tests
- Equivalent circuit
  - Temperature dependence of the coil parameters
- Conclusions

Introduction

- **Insulated coils** should be wound using tapes having **uniform electric properties**, and purchased in **long lengths** to reduce the number of resistive joints ⟶ **high costs** of the material.

- **No-insulation (NI) coils** can work properly even in the presence of defects along the tape length:

  ↓

  possible **cost reduction** of the superconducting device.

- In the scientific community, **Defect-Irrelevant windings** (DIW [1]) are presented with different perspectives: as a new winding technique or as an intrinsic feature of the existing NI technique.

- This work analyzes a single-pancake **NI High Temperature Superconducting** (**HTS**) **coil** realized with **multiple joints**, intentionally inserted between different tape lengths before the winding phase.

- **Charge-discharge cycles** are performed at different **ramp-rates**. The tests are carried out in **conduction cooling**, at temperatures between **4.7 K** and **80 K**.

- An **equivalent lumped parameter circuit** is used to retrieve the effective coil parameters.

Experimental set-up

Superconducting joints

- A **SuNAM SCN04150 tape** is selected for this work. The critical current variations along the total conductor length utilized in this work is below 1.5% ⟹ good uniformity.
- The tape lot is **cut into four segments**, re-jointed together applying a **lap joint** procedure.

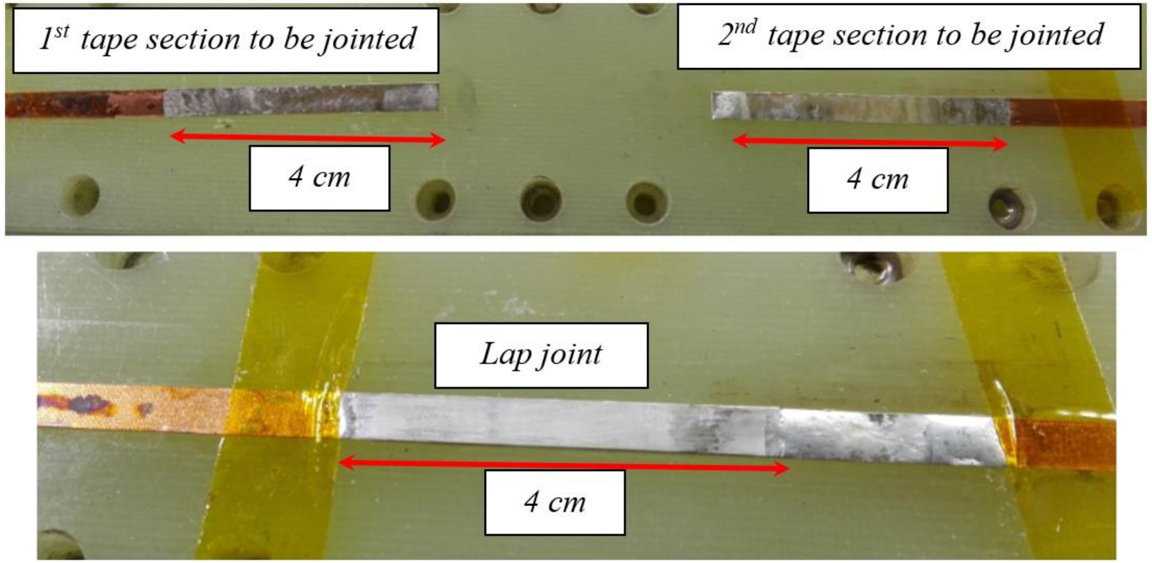

One of the lap joint realized.

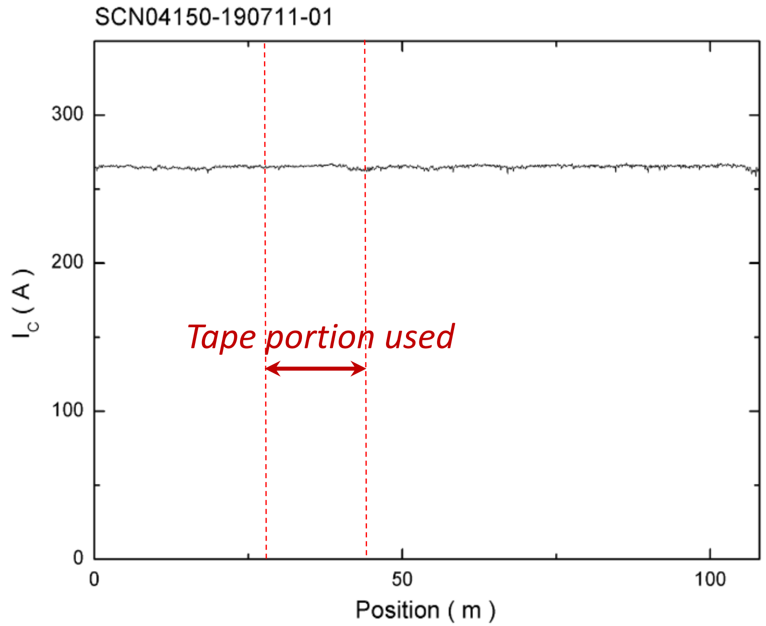

Critical current along the tape lot used in the study, provided by the manufacturer.

Experimental set-up

Superconducting joints

- The **resistance of the three joints** is measured before the winding phase and after the coil disassembly, in liquid nitrogen environment.
- One of the joints results damaged during the tests (r = 157.3 μΩ). If this **damaged section** were introduced into an insulated coil, it would require to substitute a section or the entire winding.

TAPE AND WINDING PARAMETERS

Tape width ; thickness [mm]	4.1 ; 0.145
Tape I_c ; n-value (at 77 K and s.f.)	255.4 A ; 46
Coil i.d. ; o.d. [mm]	40.1 ; 53.4
Number of layers	46
Total conductor length [m]	6.71
Length of 1st; 2nd; 3rd joint [cm]	4.0 ; 6.0 ; 8.0
Location of 1st; 2nd; 3rd joint (along the conductor) [m]	1.97 ; 3.36 ; 5.74
Resistance of 1st; 2nd; 3rd joint before winding **[μΩ·cm]**	**7.0 ; 9.0 ; 7.3**
Resistance of 1st; 2nd; 3rd joint after disassembly **[μΩ·cm]**	**8.1 ; 16.5 ; 1258.8**

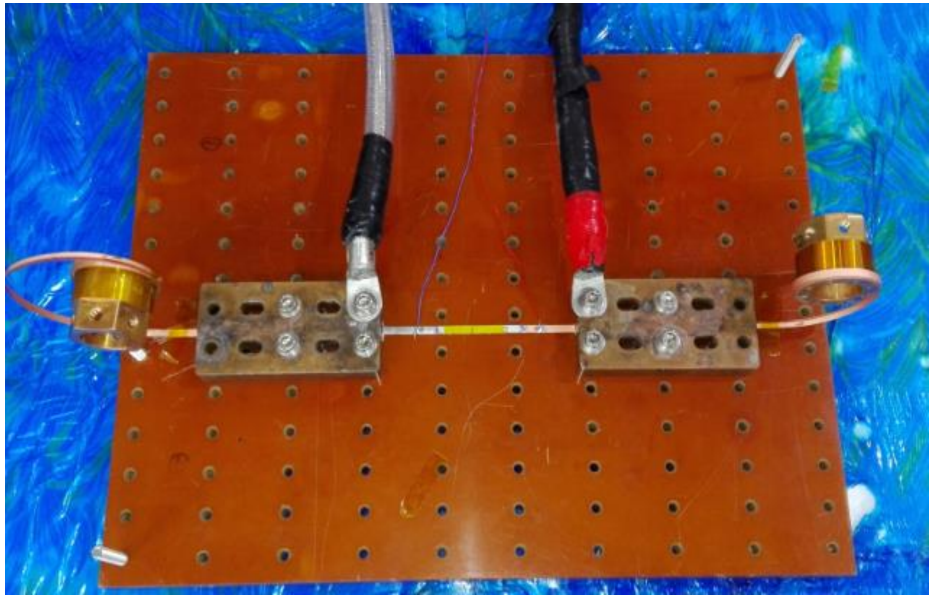

Set-up for the measurement at 77 K of the electrical resistance of one of the joints.

Experimental set-up

Winding and instrumentation phases

- The tape is wound in a **single-pancake configuration** and connected to the power supply.
- A Hall sensor is placed inside the winding bore to measure the magnetic field. A pair of voltage taps are placed at the coil ends, to acquire the voltage signal (V_{coil}) during the test phase.
- The coil is connected to the 2nd stage of a **GM crycooler** ➡ the tests are performed at different temperatures (**4.7 K** to **80 K**).

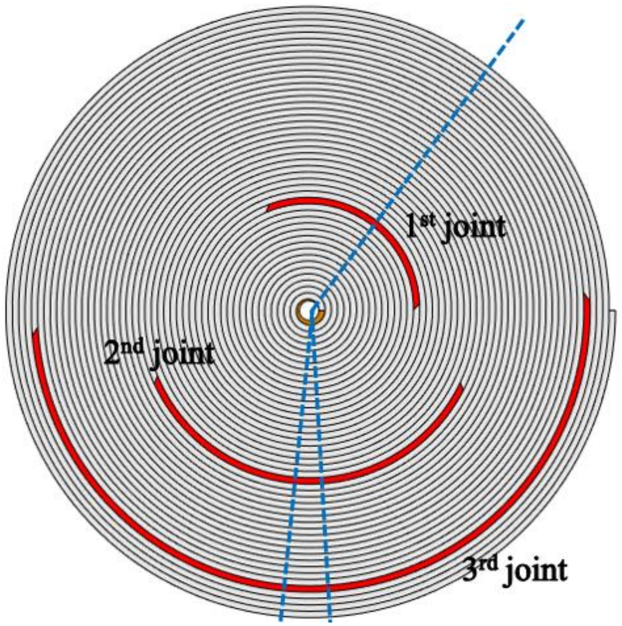

Scheme of the joints location within the coil.

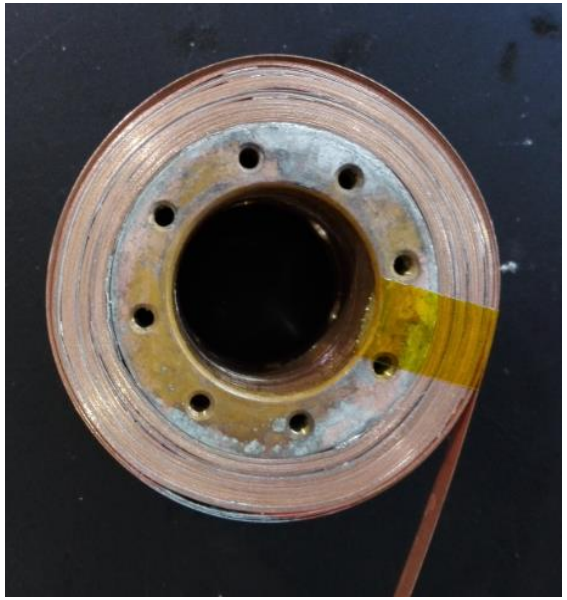

Lower view of the test coil.

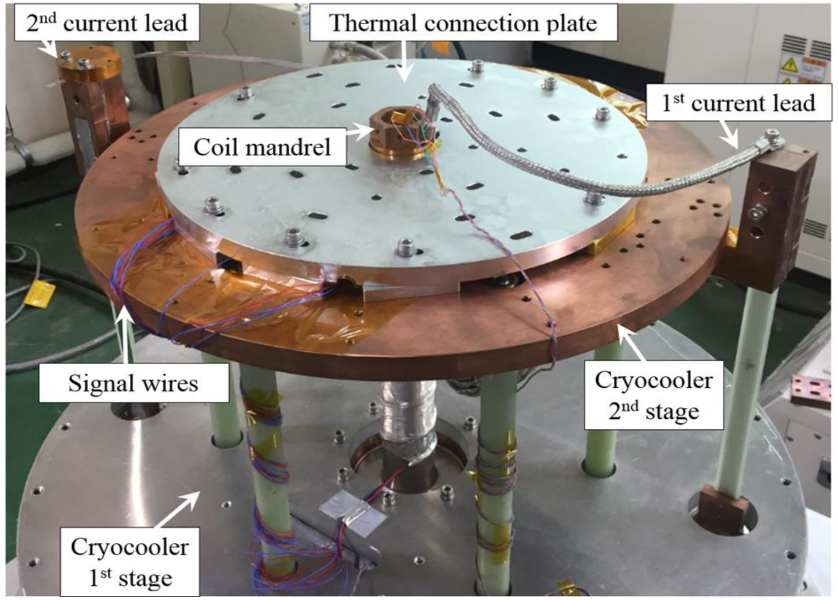

Setup for the coil connections with the cryogenic system, the power supply and the DAQ system.

Coil tests

Charge-discharge cycles

- Consecutive charge-discharge tests are performed, increasing the **ramp-rate** (0.1 A/s, 0.5 A/s, 1 A/s, 2 A/s and 5 A/s) up to the same peak current (I_{op_max} = 70 A). The temperature is varied.
- The NI coil works properly and **it can be charged and discharged safely up to rates of 5 A/s**.

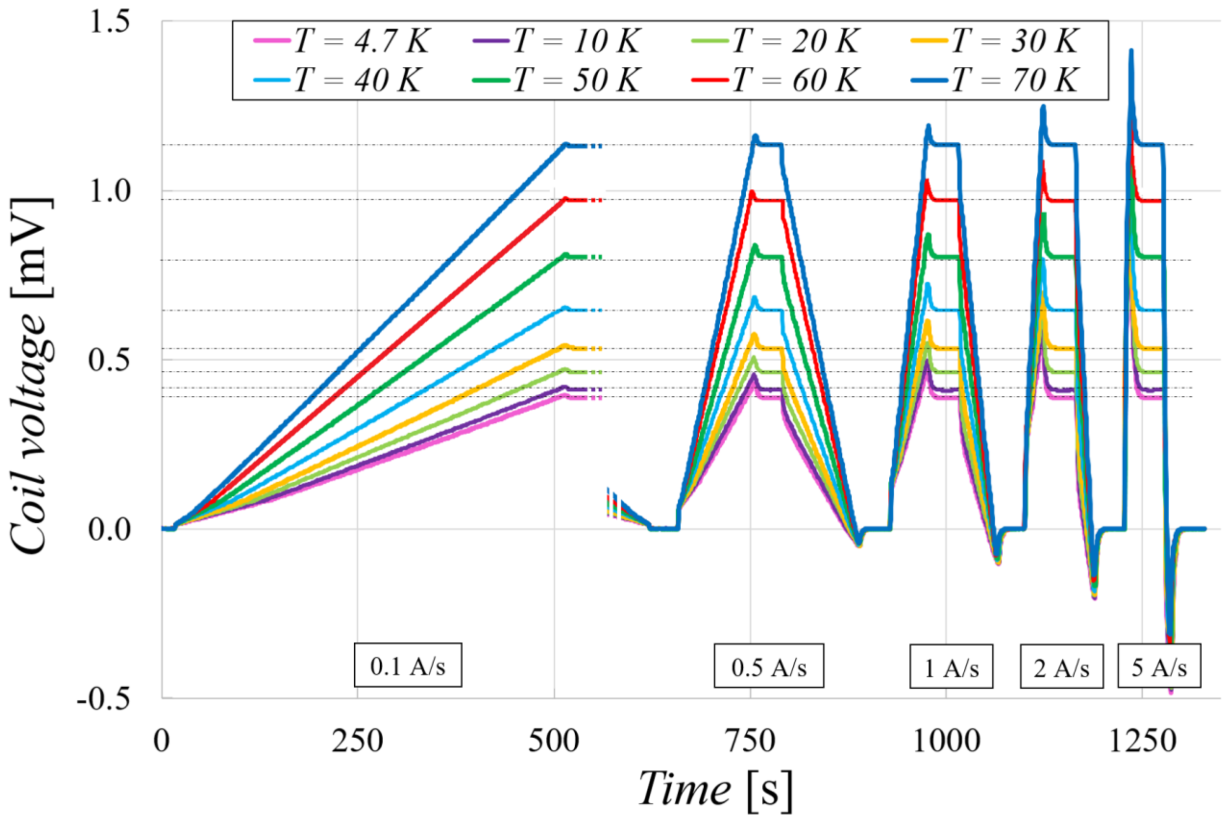

Voltage profiles measured during charging-discharging tests at different ramp-rates and temperatures.

Coil tests

Charge-discharge cycles

- The **magnetic field appears constant** with temperature and proportional to the current supplied, a sign that **the coil is performing well**, notwithstanding the presence of defects.
- However, the field results lower (~16.5%) than the one estimated analytically for a coil without defects. The difference might be due to the presence of damaged sections or small misalignments in sensor positioning.

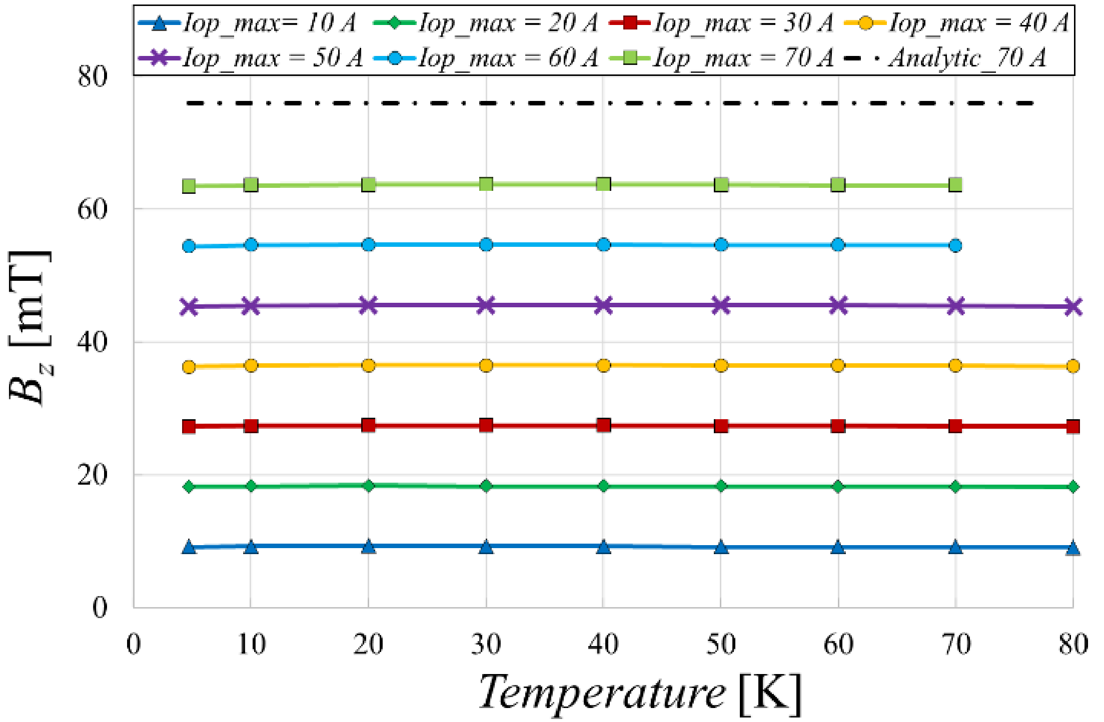

Maximum magnetic field measured during tests at different I_{op_max} values and temperatures.

Equivalent circuit

- The coil effective parameters at different temperatures are compared by means of a **simple equivalent lumped parameter circuit**. The circuit parameters are *effective* values, since they describe the macroscopic coil behavior.
- They are computed at a specific time instant t_r, when the operating current (I_{op}) equals I_{op_max} and the steady-state conditions are reached. The circuit can be simplified and **solved analytically**.

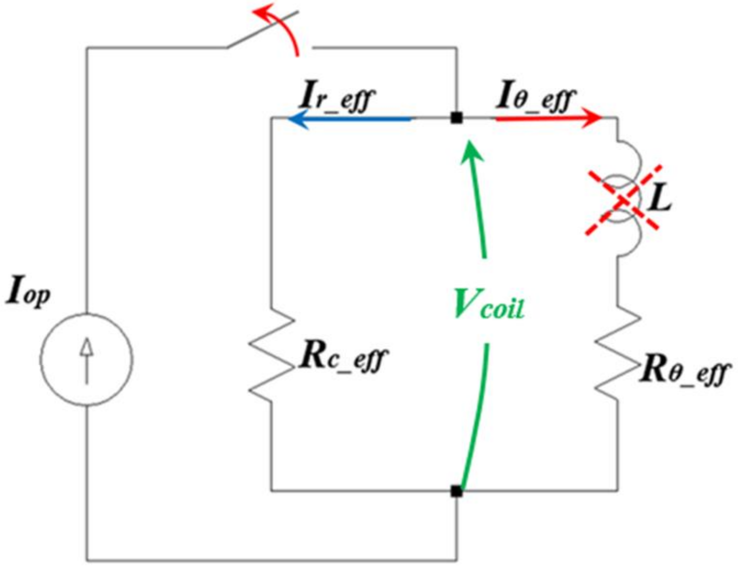

Equivalent lumped parameter circuit for a NI pancake-wound coil.

$$
\begin{cases}
I_{r\_eff}(t_r) = \dfrac{I_{op}(t_r) - \sqrt{I_{op}(t_r)2 - \dfrac{4\,\tau\, V_{coil}(t_r)\, I_{op}(t_r)}{L_{coil}}}}{2} \\
I_{\theta\_eff}(t_r) = I_{op}(t_r) - I_{r\_eff}(t_r) \\
R_{c\_eff}(t_r) = V_{coil}(t_r) \;/\; I_{r\_eff}(t_r) \\
R_{\theta_{eff}}(t_r) = V_{coil}(t_r) \;/\; I_{\theta\_eff}(t_r)
\end{cases}
$$

- I_{θ_eff} and I_{r_eff} are the currents flowing longitudinally and radially trough the coil.
- $R_{\theta_{eff}}$ accounts for the SC resistance and the resistance of the defective areas.
- R_{c_eff} is the turn-to-turn resistance of the coil.
- τ is the coil characteristic time (determined from the rapid discharge tests).
- L_{coil} is the coil inductance, computed analytically and taken equal to 150.6 μH.

Equivalent circuit

Temperature dependence of the coil parameters: τ

- In order to solve the equivalent circuit, τ is determined from the fitting of the voltage measured during the current dump.
- **τ decreases linearly with increasing the temperature**, from 832 ms at 4.7 K, to 259 ms at 80 K.

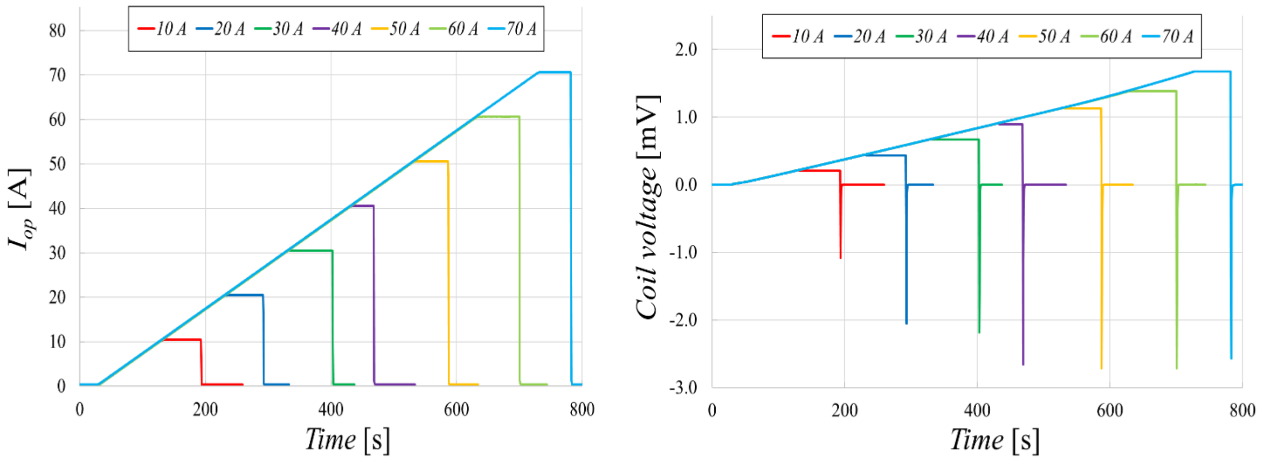

Current and voltage profiles during the rapid discharge tests at 70 K with a ramp-rate of 0.1 A/s.

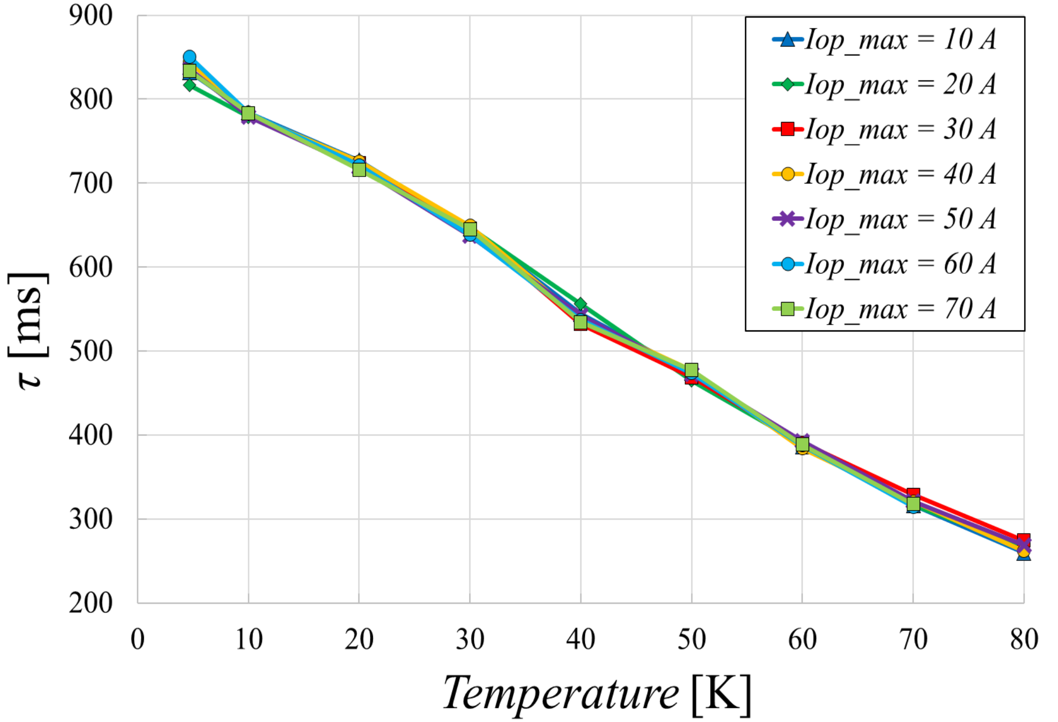

Parameter τ determined from rapid discharge tests, for different I_{op_max} values and temperatures.

Equivalent circuit

Temperature dependence of the coil parameters: $R_{\theta_{eff}}$

- **$R_{\theta_{eff}}$ increases non-linearly with temperature**. It does not correspond to the sum of the resistances measured for the 3 joints, although the order of magnitude is respected. This could be explained by a combination of two different phenomena: some tape sections might be approaching their critical current and the joint resistances also increase with temperature.

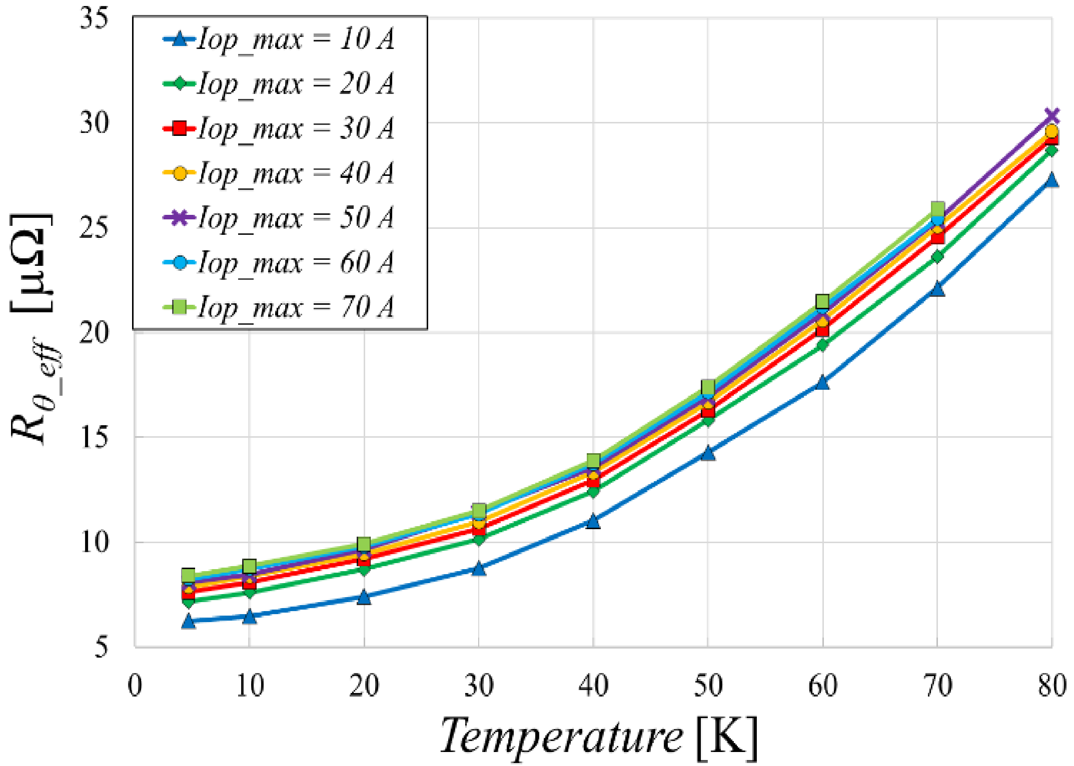

$R_{\theta_{eff}}$ computed at $t = t_r$, *for different* I_{op_max} *values and temperatures.*

Equivalent circuit

Temperature dependence of the coil parameters: R_{c_eff} and ρ_{ct_eff}

- R_{c_eff} **increases non-linearly with temperature**. The dependence resembles the copper resistivity vs temperature curve.
- The **effective turn-to-turn surface resistivity** (ρ_{ct_eff}) can be assessed using [2]: $R_{c\_eff} = \sum_{i=1}^{Nturn} \frac{\rho_{ct\_eff}}{2\,\pi\,r_i\,w}$
- The range found for ρ_{ct_eff} (from 22 μΩ·cm² at 4.7 K to 72 μΩ·cm² at 80 K) is in agreement with the values found in other publications for defect-free NI coils [3 – 8].

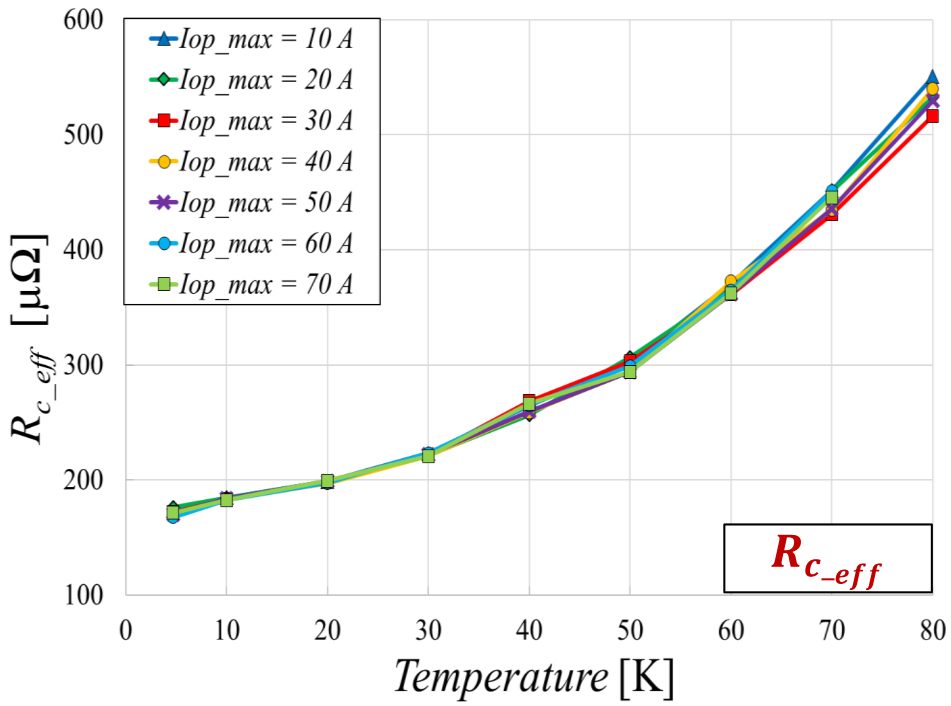

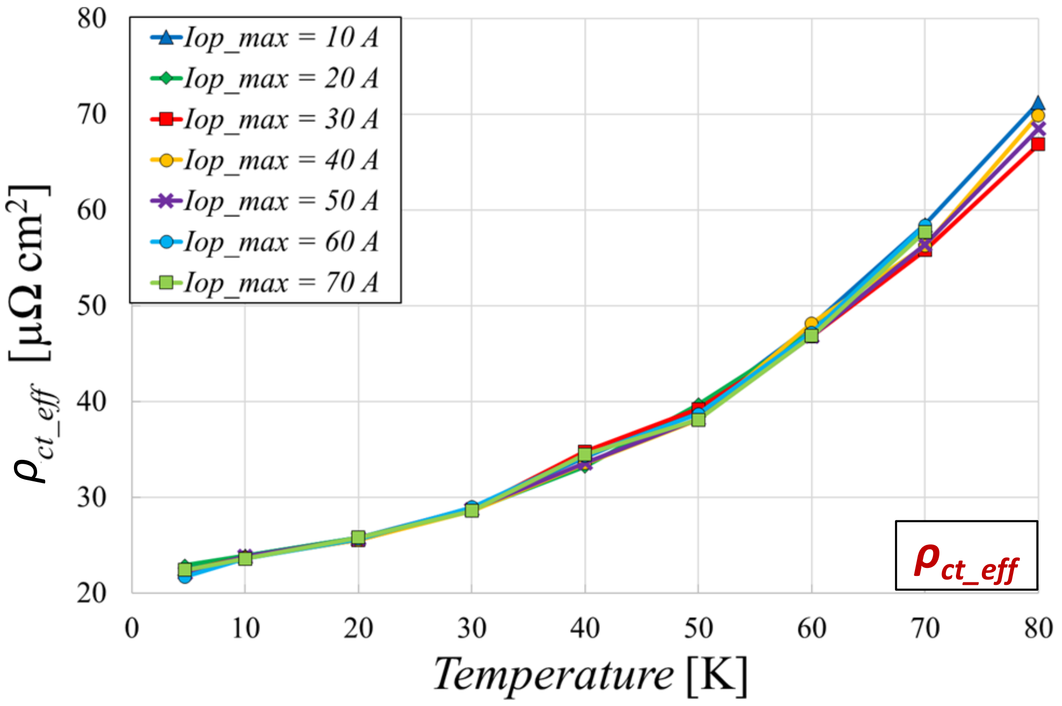

Equivalent circuit

Temperature dependence of the coil parameters: I_{r_eff}/I_{op}

- The **percentage of current flowing radially in the coil**, compared to the supplied I_{op}, **increases with the temperature**, in a range between **4.3%** and **5.5%** of the total operating current.
- In fact $R_{\theta_{eff}}$ has a steeper increase with the temperature for the same I_{op_max}, compared to R_{c_eff}.
- This agrees well with the expected behavior of NI windings, which favors the radial current flow when the longitudinal resistance rises (locally or globally), thus reducing the coil stability risks.

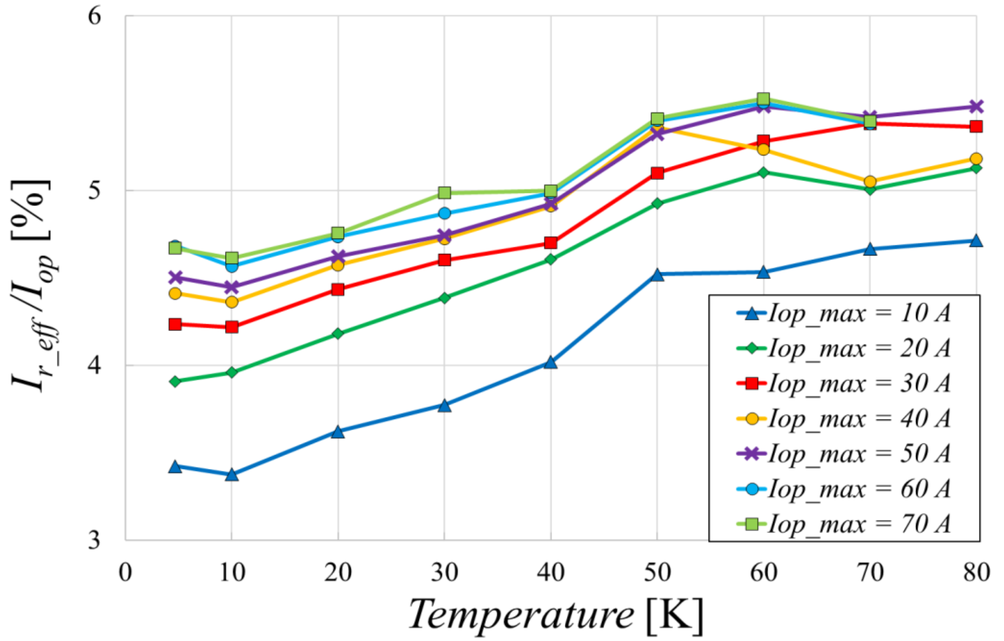

I_{r_eff}/I_{op} at $t = t_r$, for different I_{op_max} values and temperatures.

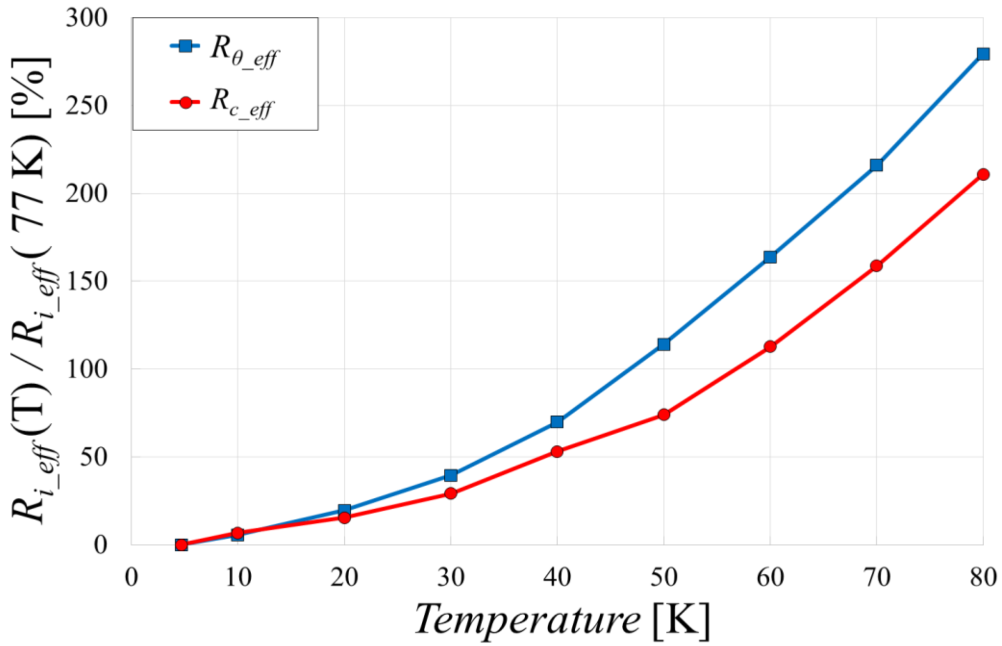

Increase with temp of $R_{\theta_{eff}}$ and R_{c_eff}, compared to the 4.7 K case.

Conclusions

- A **pancake-wound NI HTS coil** is tested in **conduction cooling** environment (**4.7 K ≤ T ≤ 80 K**), performing charge-discharge tests. Some **lap joints** are intentionally inserted into the winding at specific locations, introducing high resistance sections which would impede the operation of insulated coils.
- The test coil can be **safely charged** up to 70 A, at the maximum ramp-rate tested, equal to **5 A/s**.
- The **magnetic field measured at its bore is constant** with the temperature, although the presence of defects reduces the magnetic field compared to the one expected in a defect-free coil.
- The tests demonstrates the feasibility of winding NI coils with tape segments cut from the same lot, **potentially reducing the conductor costs** compared to the use of single long piece of tape.
- A **simple equivalent lumped parameter** circuit is adopted to analyze the electromagnetic behavior of the coil. This model allows a straightforward analytical calculation of the effective parameters of the winding at steady-state conditions, and can conveniently be applied to a quick comparison of different NI coils.
- Both **the longitudinal and radial effective resistances increase with temperature**, with the first rising more rapidly. **A quote of the operating current** (**4.3 ÷ 5.5%) flows radially through the winding**, thus guaranteeing its thermal stability.

References

[1] S. Hahn *et al., Supercond. Sci. Technol.*, vol. 29, p. 105017, Sept. 2016.

[2] X. Wang *et al., Supercond. Sci. Technol.*, vol. 26, p. 035012, Jan. 2013.

[3] M. Cho *et al., IEEE Trans. Appl. Supercond.*, vol. 29, no. 5, p. 4901605, Aug. 2019.

[4] S. An et al., vol. 31, p. 4601605, no. 5, Aug. 2021.

[5] S. Noguchi *et al., "IEEE Trans. Appl. Supercond*., vol. 29, no. 5, p. 4601605, Aug. 2019.

[6] D. G. *Yang et al., IEEE Trans. Appl. Supercond*., vol. 24, no. 3, p. 7700405, Jun. 2014.

[7] Y. Liu *et al., Supercond. Sci. Technol*., vol. 34, p. 035009, Jan. 2021.

[8] J. Lu *et al., Supercond. Sci. Technol*., vol. 31, p. 085006, Jul. 2018.